Pergamon

J. Aerosol Sci., Vol. 25, No. 6, pp. 1005–1019, 1994

0021-8502/94 $7.00 + 0.00

0021-8502(94)E0053-Z

A REVIEW OF LIQUID ATOMIZATION BY ELECTRICAL MEANS

J. M. GRACE and J. C. M. MARIJNISSEN

Delft University of Technology, Faculty of Chemical Technology, Laboratory of Particle Technology, Julianalaan 136, 2628 BL Delft, The Netherlands

(*First received* 29 *December* 1993; *and in final form* 10 *March* 1994)

Abstract—The research discipline concerning liquid atomization by electrical means is a broad discipline with a long history. As with any such discipline, communication between researchers and periodic evaluation facilitate technical progress. Complications arise when, from author to author, terminology and basic experimental techniques become incongruous and easy comparisons obviated. Several reviews on the discipline have been published that treat the historical aspects and modern research. No such review has been published since 1990. This present work focuses on post-1990 literature, not repeating the vast history.

In all, 47 reference works were investigated, of which 36 are articles concerning the atomization of liquids by primarily electrical means. As a method to show the diverse range of liquids that can be electrically atomized and to illuminate the discontinuities of data within this range, 70 liquids, as presented in the atomization references, are catalogued by reported liquid properties. The nomenclature of electrical atomization spray modes suggested by Cloupeau and Prunet-Foch (*J. Electrostatics* **25,** 165, 1990) has been continued. Three additional definitions are presented. Suggestions as to the nomenclature and unit system used, as well as the reporting of liquid properties and experimental configurations, have been made with the purpose of facilitating comparison of future experimental results.

NOMENCLATURE

EHDA	electrohydrodynamic atomization
LMIS	liquid metal ion source (or spray)
DAG	Delft aerosol generator
C	Coulombs (C)
E	electric field intensity ($V\,m^{-1}$)
S	Siemens (mho or Ω^{-1})
I	current ($C\,s^{-1}$)
L	length
M	molar
N	Newton ($kg\,m\,s^{-2}$)
Pa	Pascal ($N\,m^{-2}$)
Q	volume flow rate ($ml\,s^{-1}$)
Hz	hertz ($1\,s^{-1}$)
d	diameter
g	gravitational acceleration ($m\,s^{-2}$)
ml	milliliter (ml)
V/V	volume ratio in solution
wt	weight ratio in solution

Greek letters

α	Taylor angle (49.3°)
ε	electrical permittivity ($C^2\,N^{-1}\,m^{-2}$)
γ	surface tension ($N\,m^{-1}$)
ρ	density ($kg\,m^{-3}$)
σ	electrical conductivity ($S\,m^{-1}$)
μ	absolute viscosity (mPa s)
κ	dimensionless dielectric constant (for substance i: $\kappa_i = \varepsilon_i/\varepsilon_0$)

Subscripts

j	jet
d	diameter

1. INTRODUCTION

The possibility of using electric fields to disperse liquids has attracted much interest from the scientific community. The subject includes a wide variety of applications, numerous experimental configurations, a large array of liquids and a process that is not well understood. This leads to diverse experiments for gathering benchmark data and confusion regarding how and when given data sets can be compared.

The ubiquitous standard introduction describing the historical progress and multiple applications of the electrospray has been replaced by the pertinent definition of the electrospray and the scope of this paper. An electrospray, for the purposes herein, refers to the atomization of a liquid through the Coulombic interaction of charges on the liquid and the applied electric field. The result of this interaction includes both the acceleration of the liquid and subsequent disruption into droplets as well as the buildup of charge and subsequent disruption into droplets. This definition does not explicitly exclude mechanically assisted atomization provided that the primary atomization force remains electrical.

Here it is intended to summarize the recent literature focusing on the period from 1990 to the present. Several notable works on the field of electrospraying of liquids provide a thorough treatment of the subject: Kozhenkov and Fuks (1976), Bailey (1988), Michelson (1990) and Cloupeau and Prunet-Foch (1990). Since 1990 little has been done to this end. Within the given focus, the paper presents the experimental results in terms of their extension to the range of the electrospray technique. Some modelling and numerical methods are discussed to present the current level of this research rather than to evaluate and compare the works. The great body of literature concerning the stability of liquid jets or electrosprays in general has been left alone.

The nomenclature of electrosprays will be addressed. Focus will be on the definition of specific modes of the electrospray. These models are defined by experimentally observable differences, both visual and measurable. The transitions between modes are not always clearly defined and gray areas or overlap regions exist. These are considered but not rigorously analyzed. This paper serves as a guide rather than a rule for electrospray nomenclature of future papers.

In this light, the first definition will be presented here, followed by others in Section 2.1. The electrospraying of liquids herein is referred to as electrohydrodynamic atomization (EHDA). Both terms have merit and cross-overs to work not consistent with the scope of this paper; however, the atomization by primarily electrical (electro) forces of a liquid (hydro) that is moving (dynamic) during the atomization captures the essence of the phenomena. That motion applies to the liquid, however small, results from the production of droplets and the consequential mass transfer. Electrostatic spraying can apply to non-electric phenomena, e.g., paint sprays where the atomization by mechanical forces dominates and the subsequent charging (by induction or ion transfer) results in a charged aerosol. This does not fit the area under consideration. Certainly, electrohydrodynamic does not imply droplet investigation *per se*, but the term electrohydrodynamic atomization (EHDA) applies to the subject.

The process of EHDA can take place in various atmospheres (air, inert gas, vacuum, etc.) using various fluids and experimental conditions, and generate droplets from various production mechanisms (single jet, multiple jets, emission, collapse, etc.). This process includes the production of charged droplets all the way from field enhanced dripping to rim emission, from the production of large (order of mm) to very small (order of nm) droplets, from polydisperse to monodisperse droplet populations, and from low to high flow rates.

At present, no complete theory exists that describes how the atomization process proceeds as a function of operation conditions, both external (experimental configuration, flow rate and atmosphere) and internal (fluid properties). The fluid properties receiving the most attention are: the electrical conductivity (σ), the surface tension (γ), the absolute viscosity (μ), the density (ρ) and the dielectric constant (κ).

The format of this article follows as a presentation of available data reviewed, a discussion on the current nomenclature for the spray modes with additions to this list, and by a brief

section on the current analytical and numerical modelling of EHDA. A summary and suggestions for future EHDA works and articles concludes the review.

2. PRESENTATION OF DATA

The value of the liquid properties compiled from the reviewed papers (σ, γ, μ, and ρ) are listed in Table 1. Here an $\times$ denotes unreported values and an * denotes values found by the reviewers in CRC (1982). The liquids are listed alphabetically with a liquid reference number and an author reference number. The liquid reference number is provided for convenience and the author reference number refers to the bibliographic location of the reporting author(s). Several authors may have experimented with a given liquid. In this case, each line refers to a specific author, as indicated by the author reference number. Figure 1 details the range of reported flow rates. This figure shows the wide range of flow rates for EHDA, spanning several orders of magnitude. Note that these values represent the reported extent that EHDA, can be used for liquid dispersion. It does not distinguish between particular EHDA modes and the restrictions these entail. Similar plots can be constructed from the data in Table 1 to show the vast extent of liquid properties investigated.

Some values for a given liquid and property listed in Table 1 exhibit a large difference, e.g., water (pure) used by Cloupeau and Prunet-Foch (1990) ($\sigma = 2.5 \times 10^{-4}\ \mathrm{S\,m^{-1}}$) and water (distilled) used by Balachandran *et al.* (1992) ($\sigma = 2.5 \times 10^{-2}\ \mathrm{S\,m^{-1}}$). This reflects the different processing methods, e.g., number of distillation cycles, and does not warrant a new liquid category. The uncertainty in the values can be seen by the variations in the properties of the same liquid as measured by different authors, e.g., Smith (1986) reports ($\sigma = 6 \times 10^{-6}\ \mathrm{S\,m^{-1}}$) for glycerol and Kirichenko *et al.* (1990) report ($\sigma = 3.3 \times 10^{-6}\ \mathrm{S\,m^{-1}}$). Liquids, when categorized by electrical conductivity, are, in general, referred to as low, moderate or high conductivity liquids. Numerically, moderate conductivity liquids fall in the range of 10^{-4}–$10^{-8}\ \mathrm{S\,m^{-1}}$. High and low conductivities bracket this range.

The range of external parameters found in the literature, namely the liquid flow rate and the experimental configuration are now discussed. Note that the experimental configurations generally have either constant flow or constant pressure sources. The parameter of interest for a review is the flow rate. The hydrostatic pressure force can be useful for a force balance on the liquid; however, the magnitude is usually small relative to the electrical forces and reverts to a low flow rate condition.

Generally, the flow rate limits are experimentally imposed rather than physically limited. Atomization at low flow rates is predominately the domain of nanoparticle fabrication and mass spectrometry (e.g., Loscertales and Fernández de la Mora (1993) and Hiraoka (1992)). These two processes take advantage of the small size droplets produced by EHDA and further reduce the size by evaporation of the solvent liquid. Similarly, the high flow rate systems appear limited by experimental constraints such as rapidly concentrating sufficient charge in the liquid and achieving the high electric field intensities necessary to create an electrical force greater than the mechanical forces of fluid motion.

The total or effective electric field at the production site is the vector sum of the external electric field or that due to the experimental configuration, and the internal electric field or that due to the space charge. The concentration of the total electric field depends primarily on the limitations of the medium (dielectric strength), the electrical configuration and the space charge.

Several types of electrical configurations are reported in the literature. The high field intensities necessary for EHDA are achieved easily by concentrating the electric field to a small region, e.g., the tip of a capillary. The capillary-plate configuration, as it is the most common EHDA configuration reported, leads us to define the capillary-plate configuration as the benchmark or standard experimental configuration. Other configurations certainly exists and, depending on the application, perform better than the capillary-plate configuration; however, for this review the capillary-plate configuration serves as the standard. Variations on this theme include constant pressure versus constant flow sources; liquid flow

Table 1. Catalogue on reported liquid properties

Liquid reference number	Liquid	Conductivity ($S\,m^{-1}$)	Surface tension ($N\,m^{-1}$)	Absolute viscosity (mPa s)	Density ($kg\,m^{-3}$)	Author reference number
1	Acetone	×	0.025	*0.316	*1432	41
2	Butanol	×	0.025	*2.95	*810	41
3	Cyclohexane with	6.8E − 06	0.032	260	×	27
	MCH copolymer	3.9E − 04	0.032	260	×	27
4	Cyclohexanol	2.1E − 06	×	68	×	5
		×	×	55	960	40
		2.8E − 04	0.033	58	×	27
5	Dibutyl phthalate	×	0.028	×	×	41
		2.1E − 06	0.035	25	×	27
		×	×	21	1040	40
6	Dibutyl phthalate with triethylene glycol	1.5E − 07	×	24	×	5
7	Dichloroethane	2.0E − 04	0.034	20	×	27
	with perchlorovinyl	1.0E − 02	0.034	×	×	27
8	Dichloroethane	5.0E − 04	0.034	50	×	27
	with polystyrene	5.0E − 03	0.034	400	×	27
9	Diethyl phthalate	×	0.04	×	×	41
10	Diethyl sebecate	2.0E − 08	×	7	×	5
11	Digol	×	0.046	×	×	41
12	Dimethylacetamide with polyacrylonitrile	2.4E − 03	0.04	6400	×	27
13	Dimethyl phthalate	×	×	16	1190	40
		3.8E − 06	0.033	58	×	27
14	Ethanol	1.0E − 05	0.023	1.2	×	5
		×	0.024	×	×	41
		2.0E − 05	0.02275	1.2	789	7, 8, 16, 17, 39
		×	×	×	×	36
		7.0E − 06	0.0277	×	×	31
15	Ethanol with BF-2 glue	2.0E − 03	0.022	20	×	27
		8.0E − 03	0.022	600	×	27
16	Ethanol with DOP	×	×	×	×	32
17	Ethanol with	2.2E − 03	0.022	120	×	27
	polyvinylpyrolidane	2.2E − 03	0.022	1000	×	27
18	Ethanol with $Sn(Ac)_4$	×	×	×	×	46
19	Ethyl benzoate	5.0E − 07	×	2.24	×	5
20	Ethylene glycol	×	0.05	×	×	41
		×	0.0463	×	*1108	32
21	Formamide with dioxane	3.2E − 07	×	×	×	4
		3.6E − 05	×	×	×	4
22	Formamide with 1 M LiCl	1.3E + 00	0.0376	1.804	1134	10
23	Freon 113 ($C_2Cl_3F_3$)	6.0E − 08	0.019	0.64	1565	25
24	Glycerol	×	0.063	1490	1261	30
		6.0E − 06	0.063	×	×	41
		3.3E − 06	0.062	1300	×	27
		×	×	1300	1260	40
		×	0.063	×	1260	37
25	Glycerol with NaI	×	×	×	×	9
	(3, 5, 7.1% wt)	×				
	(10% wt)	×	×	×	×	30
26	Glycerol with NaI (10% wt)	×	×	×	×	30
	with dodecyl sulfate (0.1% wt)	×	×	×	×	
27	Heptane with ? (0.3% wt)	×	×	×	×	14
	Heptane with stedis 450 (0.3% wt)	1.2E − 06	0.018	0.61	×	15
28	Hexane	1.0E − 11	*0.0184	*0.362	*659	41
29	Isopar M	1.0E − 12	×	×	×	18
30	Isopar M with	3.1E − 11	×	×	×	18
	Butanol (5%)		×	×	×	18
31	Butanol (10%)	6.7E − 10	×	×	×	18
32	Butanol (15%)	7.1E − 09	×	×	×	18
33	Butanol (20%)	3.9E − 08	×	×	×	18
34	Butanol (25%)	1.3E − 07	×	×	×	18
35	Butanol (30%)	4.0E − 07	×	×	×	18
36	Butanol (35%)	1.3E − 06	×	×	×	18
37	Butanol (40%)	2.2E − 06	×	×	×	18
38	Butanol (45%)	3.1E − 06	×	×	×	18
39	Butanol (50%)	4.5E − 06	×	×	×	18

Table 1. *Continued*

Liquid reference number	Liquid	Conductivity ($S\,m^{-1}$)	Surface tension ($N\,m^{-1}$)	Absolute viscosity (mPa s)	Density ($kg\,m^{-3}$)	Author reference number
40	Jet A	3.0E − 13	×	×	×	23, 24
41	Marcol 87	×	×	2	×	23, 24
42	Methanol	×	*0.0226	*0.597	*791	14
43	Methanol with glycerol (75:25% V/V)	×	×	×	×	30
44	Methanol + water + CCl_4 (8 : 2 : 0.5 V/V) with 5E−06 M (CH_3) 4NBr and with 1E−03 M CH_3COOH	×	×	×	×	19
45	Methylchlorophorm	7.0E − 04	0.028	300	×	27
	with perchlorovinyl	7.0E − 04	0.028	700	×	27
46	*n*-Octanol	×	*0.0275	*0.542	*821	39
47	*n*-Octanol with H_2SO_4 (5% V/V)	5.0E − 02	×	×	×	10
48	Octoil	×	0.031	×	980	37
49	Propanol	×	×	×	×	20
		5.0E − 05	0.022	*2.256	*780	41
50	Propanol with HCl (0.05%)	1.1E − 04	×	×	×	41
51	HCl (0.125%)	1.2E − 03	×	×	×	41
52	HCl (0.25%)	1.4E − 02	×	×	×	41
53	HCl (0.5%)	1.0E − 01	×	×	×	41
54	Propanol with NaI (0.618 gml^{-1})	6.8E − 03	0.0238	×	×	38
55	Tin, superheated	×	0.4	*0.6	7000	48
56	Toluene	1.0E − 11	*0.0285	*0.59	*867	41
57	Water	2.5E − 04	0.0289	*1	*1000	5
		2.5E − 02	×	×	×	2
		1.2E − 04	0.073	×	×	41
		3.0E − 01	×	1	1000	18
58	Water with 2% Hodag 1035L	×	0.0425	×	×	41
59	Water with 0.5% Hodag	2.2E − 02	0.044	0.95	×	41
60	Water with 0.5% Hodag with glycerol (33%)	×	×	3.28	×	41
61	with glycerol (50%)	×	×	7.4	×	41
62	with glycerol (60%)	×	×	16.6	×	41
63	with NaCl (0.01%)	6.0E − 02	0.044	×	×	41
64	with NaCl (0.05%)	2.9E − 01	0.044	×	×	41
65	with NaCl (0.1%)	5.0E − 01	0.044	×	×	41
66	Water with polyethylene oxide	1.1E − 02	0.072	150	×	27
67	Water with polyvinyl alcohol	2.0E − 02	0.072	800	×	27
		2.7E − 02	0.072	800	×	27
68	Water–limestone slurry	×	×	×	×	49
69	Woods metal	×	0.045	×	970	37
70	Zirconia precursor solution	1.11E − 00	×	×	×	2

through versus around the electrode; geometrical variations in the reference electrode, e.g., a disk with a hole for sampling, a collection cup, etc.; and variations in the number of electrodes, e.g., a third electrode within the electric field. Other electric field configurations resulting from adjacent sprays are noted (Snarski and Dunn, 1991; Rulison and Flagan, 1993) but not discussed.

The general parameters varied in the electric configuration are the electrode dimensions and inter-electrode spacing. These variations allow for different external electric field intensities given similar applied voltages and liquid properties. The total electric field intensity at the production site controls EHDA.

Calculation of the total electric field intensity at the production site is difficult. Analytical models have been developed to approximate the external electric field for the capillary-plate configuration (Jones and Thong, Van Dyke, Loeb *et al.*: as referenced by Smith 1986), but other configurations must rely on numerical modelling. Any technique, analytical or numerical, requires information on the space charge modulation of the field intensity to

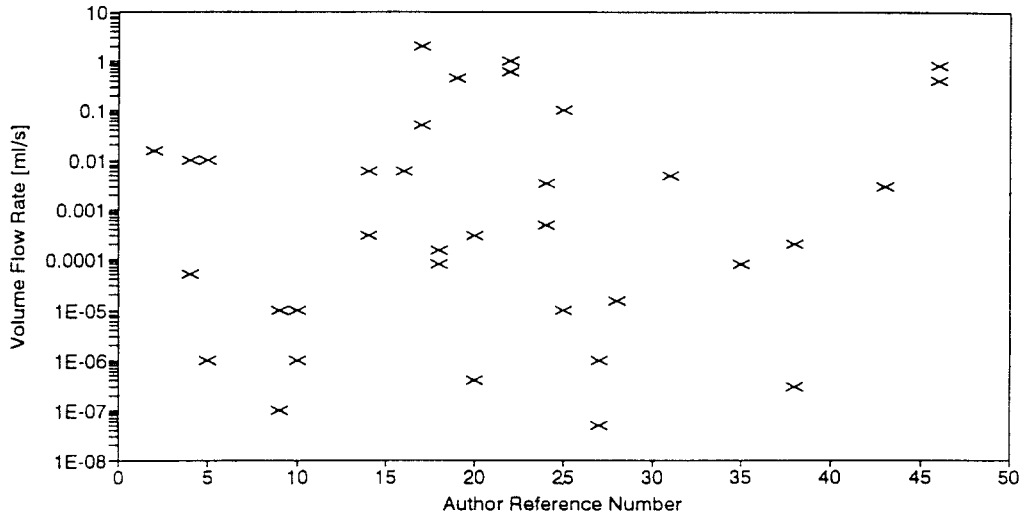

Fig. 1. Experimental flow rate data.

accurately predict the total electric field intensity at the atomization site. This effect of the space charge (due to charged droplets, corona discharge or ion emission) is not well understood.

2.1. *Spray modes*

EHDA, for constant liquid properties and flow rate, progresses through several visual and measurable differences with increasing applied voltage. These differences are defined as spray modes. The particular spray mode achieved depends on the operating conditions of the experiment.

Several spray modes have been defined by Cloupeau and Prunet-Foch (1990) and these definitions have been continued here. A brief summary of these spray modes is given in the following. Note that each mode has multiple characteristics and the transition between modes is not always well defined; consequently, the simple descriptions to follow cannot fully encompass the subtleties of each mode. Figure 2 presents a flow chart describing the modes as a function of the applied potential. Here it is not meant to imply that all liquids under all conditions will follow identically, without deviation, the mode progression through potential space. However, this figure, in general, locates the modes described below in the potential space of the spray.

The modes are separated into two general categories: those that exhibit a continuous flow of liquid through the meniscus and those that do not. The former consists of the simple-jet, the cone-jet and the ramified-jet, while the latter consists of the dripping, the microdripping, the spindle and the intermittent cone-jet modes. The latter modes are often referred to as pulsating modes. Both categories have been observed by most authors although the nomenclature has not been universally accepted.

The dripping mode is characterized by the production of large droplets (usually larger than the capillary diameter) at low frequency ($<$ about 500 Hz). The production frequency and the droplet diameter vary directly and inversely, respectively, with the applied potential. The primary droplets are sometimes accompanied by satellite droplets. The microdripping mode occurs at low flow rates and produces droplets smaller than the capillary diameter at a frequency about two orders higher than the dripping mode. The spindle mode generates two distinct droplet sizes, a large primary droplet and several small satellites. In this mode, a jet extends from the meniscus and collapses into the primary and satellite droplets. The meniscus collapses to the capillary tip and the process is repeated with a regularity depending on the conditions. The intermittent cone-jet mode, as the name suggests,

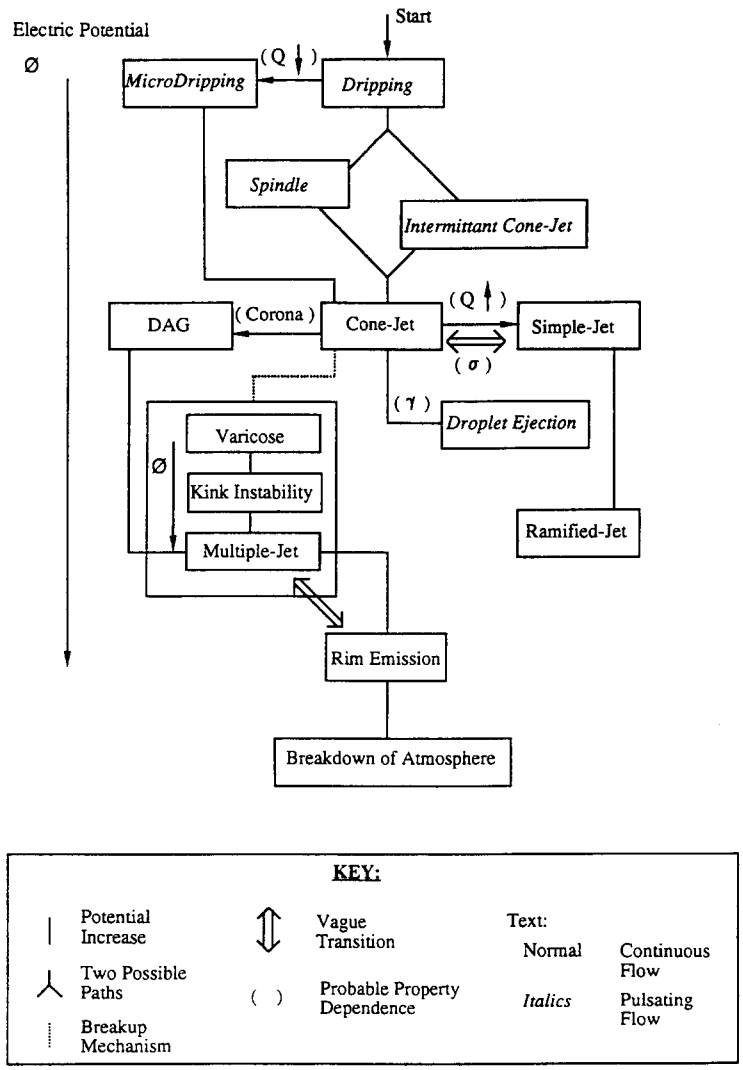

Fig. 2. Flow chart of spray modes in electric potential space.

produces an unstable cone-jet. Between the cone-jet occurrences the meniscus collapses to the capillary and several large droplets may be emitted. Previous nomenclature has grouped the spindle and the intermittent cone-jet modes into one mode, the pulsating-jet mode. The droplet diameter differentiates the two modes. The spindle mode produces two diameter classes where the intermittent cone-jet mode produces a multitude of fine droplets with a superimposed, semi-periodic large droplet population.

The continuous modes are described in the following. The simple-jet and cone-jet exhibit similar structures. The transition between the two is sharp for high conductivity liquids and vague for low conductivity liquids. Both consist of a single jet drawn from the meniscus by the electrical forces. In the cone-jet mode, often referred to as the Taylor cone mode, the meniscus forms a conical shape with a half angle near the 49.3° Taylor angle (as calculated from an ideal, no-flow equilibrium condition). The jet drawn from the apex of this meniscus breaks up into droplets by three mechanisms as a function of increasing potential: varicose instabilities where the breakup proceeds as in a natural jet, kink instabilities where the breakup is more disordered due to the large lateral instabilities caused by the high electric forces and lastly, the multi-jet instability where multiple jets appear on the meniscus and the jet length is shorter. The simple-jet differs from the cone-jet in the sharpness of the conical meniscus and in this mode breakup usually occurs via varicose instabilities. The ramified-jet

occurs at higher flow rates and is characterized by one or more jets issuing from the capillary tip and several temporal secondary jets issuing from the surface of the primary jet(s), not just the apex.

2.2. *Literature review*

The focus of the following spray mode review is a supplement and an extension to the Cloupeau and Prunet-Foch (1990) nomenclature for the works from 1990 to the present.

The single most common spray mode reported is the cone-jet mode. Consequently, works concerning this mode will be reviewed first. Of the papers, one reported experiments done exclusively under vacuum conditions (Vladimirov *et al.*, 1993). This paper detailed a liquid metal ion spray or source (LMIS) which usually does not fall under the heading of EHDA. However, the mechanism is primarily electrical and, therefore, has many similarities to the standard EHDA and should be considered (Forbes and Ljepojevic, 1991a). The liquid used was superheated tin with an estimated surface tension of 0.4 $N\,m^{-1}$ which is considerably higher than most liquids reported. No flow rate or liquid properties were reported. The electric configuration in this experiment had an extruder electrode typical of liquid metal sprays. The generated droplets were on the order of $1–10^3$ nm.

The remaining cone-jet papers can be further sub-divided by flow rate into two categories: high ($>10^{-5}$ $ml\,s^{-1}$) and low ($<10^{-5}$ $ml\,s^{-1}$). The relatively high flow rate conditions achieved by Meesters *et al.* (1992) and Vercoulen *et al.* (1993) ($Q\sim 1\times 10^{-3}$ $ml\,s^{-1}$) involved a submode which does not fall into the classes previously mentioned. This mode exhibits a Taylor-like cone, but no visible jet. In addition, a corona discharge near the cone apex is reported as a necessary condition and a ring electrode and an electrically-grounded needle modify the electrical configuration. This mode achieves a very high droplet production frequency, on the order of 10^8 Hz for diameters ~ 1 μm. The production frequency coupled with the necessary corona differentiate this mode from the cone-jet mode. Therefore, this mode is termed the space charge controlled regime of the Taylor cone, or the Delft Aerosol Generator (DAG) mode. Note that there has been much discussion on the existence of a jet and the mechanism by which droplets are produced. In this mode it has been resolved that the mechanism is not well understood and that it is different than the cone-jet mode.

Balachandran *et al.* (1992) have achieved a stable cone-jet for high flow rates ($Q\sim 1\times 10^{-2}$ $ml\,s^{-1}$) and a highly conducting fluid (water and a zirconia precursor solution) using an AC superimposed field on a DC base potential.

Gomez and Tang (1990) report on spraying methanol and doped heptane at flow rates from 10^{-5} to 10^{-4} $ml\,s^{-1}$. These experiments were conducted with a constant flow rate source with a capillary-plate configuration. The authors also observed the pulsating mode and breakup by kink instability, consistent with Fig. 2. Satellite and primary droplets were observed under breakup by varicose instability, but Coulomb fission was not reported. The spray was characterized for application to combustion processes by measuring both the droplet diameter and velocity through the spray and calculating evaporation rates. The authors conclude from the velocity data and a reduced momentum equation that the droplet velocity and the total electric field monotonically decrease with axial position from the liquid meniscus. This conclusion is, in general, not true as the image force results in a droplet acceleration near the plate (Grace, 1993; Gañán-Calvo *et al.*, 1994). The liquid properties are not reported in this work.

A later work by the same authors, Gomez and Tang (1994), uses the capillary-plate configuration with a constant pressure source and flow rates varying from $\sim 7\times 10^{-5}$ to $\sim 2\times 10^{-2}$ $ml\,s^{-1}$. This study also uses doped heptane and the properties are well reported. The dopant in the previous work is presumably the same (Stadis 450, 0.3% by wt). The authors investigated droplet disintegration due to electrical surface instability or Coulomb fission. Some excellent photographs of droplets during this process are presented. The results suggest that Coulomb fission occurs at 70–80% of the Rayleigh limit. Aerodynamic effects are assumed to account for the difference from the ideal limit. It is interesting to note that the

data reported on specific charge versus droplet diameter follows an opposite trend to that reported for octoil by Hendricks in Pfeifer and Hendricks (1967) for the same spray mode but with generally different diameter droplets.

In the low flow rate conditions both Fernández de la Mora (1992) and Rulison and Flagan (1993) produce sprays to study their electrical properties. Respectively, these authors study the space charge effects and the juxtaposing of capillaries. These sprays typically generate monodisperse droplets on the order of a micron and below. Fernández de la Mora (1992) used octanol doped with 5% H_2SO_4 at flow rates $\sim 5 \times 10^{-6}$ ml s^{-1} and Rulison and Flagan (1993) used *n*-propyl alcohol at flow rates $\sim 1 \times 10^{-5}$ ml s^{-1}. Hiraoka (1992) studied the desorption characteristics of charged droplets by coupling an EHDA source and a mass spectrometry measurement system. These experiments were conducted with 5×10^{-6} M $(CH_3)_4NBr$ and 1×10^{-3} M CH_3COOH in a mixture of $CH_3OH + H_2O + CCl_4$ (8:2:0.5, V/V) at flow rates $\sim 1 \times 10^{-5}$ ml s^{-1}. He took advantage of the droplet evaporation to study ion products. Loscertales and Fernández de la Mora (1993) generated nm size particles using formamide doped with 1 M LiCl at a flow rate of $\sim 1 \times 10^{-7}$ ml s^{-1} for testing a hypersonic impactor for aerosol measurements. Fernández de la Mora *et al.* (1990) generated submicron monodisperse droplets using glycerol doped with NaI (3 – 7% by wt) at a flow rate of $\sim 1 \times 10^{-6}$ ml s^{-1}.

The remaining reviewed references dated 1990 or later do not primarily work with the cone-jet mode. Kirichencko *et al.* (1990) investigated spray transported electric currents and the specific electric charge in C m^{-3} for 3 monomer Newtonian liquids and 9 polymer solutions (see Table 1). The electrical configuration differed from the standard capillary-plate configuration in that a third electrode surrounded the capillary. This electrode and the liquid were charged with a negative DC voltage. Two orientations for the capillary were used: "up", such that the jet was drawn out in the opposite direction to the gravity vector and due to the allowed flow between the capillary and the third electrode, represented a constant pressure source; and "down", such that the jet operated in the same direction as the gravity vector and was controlled by a constant volume flow rate source. The reported observations indicate operation in the simple-jet mode for all conditions studied.

Wang *et al.* (1993) investigated EHDA of a limestone–water slurry as an alternative to the currently used compressed gas atomization. No properties are reported and the flow rates are between 0.4 and 0.8 ml s^{-1}. A capillary-collection tank with a negative DC voltage source is used. The reported spray consists of two parts: a continuous filament and spread droplets. Photographs of the spray show similarities with the ramified-jet where secondary emission sites exist off the primary jet. The produced droplets vary from 100 μm to more than 2 mm. The diameter probability distribution function has a bimodal character where the small peak is associated with the secondary emission and the larger peak with the primary jet.

Two references involve morphological studies of EHDA using distilled water and glycerol solutions. Jaworek and Krupa (1992) studied the EHDA of water using a capillary-plate configuration with both positive and negative DC voltages. The flow rate is not reported, but the experimental apparatus is set up with a constant pressure source such that no dripping is observed without the electric field. Therefore, the flow rates, based on a similar apparatus described by Smith (1986) is estimated to be on the order of 10^{-5} ml s^{-1}. This study shows excellent photographs of several spray modes including the dripping mode, the spindle mode and the cone-jet mode (with breakup by multiple jets and kink instabilities). These photographs are taken with short duration (1.5 and 3 μs) and long duration (1/30 s) exposures. The results indicate that EHDA is far from an ideal process and can be quite messy. Also shown are photographs of rotation of the jet about the axis of the capillary in the cone-jet mode as briefly mentioned by Cloupeau and Prunet-Foch (1990).

Lüttgens *et al.* (1992) investigated EHDA of glycerol solutions for the use with mass spectrometry measurements. The apparatus consisted of a capillary-plate with a positive DC voltage under both vacuum and air atmospheres. The flow rates were less than 1.5×10^{-5} ml s^{-1}. The experiments, run under vacuum conditions, show evolution of the spray through the dripping, the pulsating-jet (the intermittent cone-jet), the cone-jet and the rim emission modes with increasing applied potential. Doping the glycerol with NaI (10% by wt)

did not change the evolution, but finer jets were produced in the cone-jet and the rim emission modes. Pulsed ion emissions, which could not be resolved with flow visualization, were measured using mass spectrometry in the rim emission mode. Addition of the suffricant dodecyl (0.1% by wt) to the doped solution lowered the onset voltages in the cone-jet and rim emission modes, but did not otherwise change the observations. Experiments conducted under an air atmosphere using pure and doped glycerol (with NaI) showed no qualitative differences from the vacuum results for voltages less than the rim emission mode. Under air no rim emission mode was observed, rather a droplet ejection mode where liquid leaving the capillary was ejected as large droplets succeeded the cone-jet mode. As a result of this work, two additional modes are included in the spray nomenclature: the droplet ejection mode and rim emission mode.

The droplet ejection mode, as described, appears similar to some pulsating modes; however, its occurrence at a higher potential than the cone-jet mode and the large droplet size differentiates it from the pulsating modes. This mode was not reported to depend on the liquid viscosity. It was, however, reported to be influenced by the surface tension. Additional experiments conducted using a glycerol/methanol solution (25:75 V/V) rather than pure glycerol show the rim emission mode succeeded the cone-jet mode with increasing potential. The atmospheric pressure was assumed to act to stabilize the meniscus leaving the capillary such that a convex meniscus formed and the flow was not completely regulated by the electrical forces, as in the vacuum case (concave meniscus). The reported production frequency of droplet ejection was low, on the order of 10 Hz.

The rim emission mode has many similarities to the multiple cone-jet mode where the number of jets is large (> 5). In this mode, the cone disappears and the droplets seem to be emitted directly from the capillary tip. This mode can be seen as a limiting case of the multiple cone-jet mode. Multiple jets in the cone-jet mode imply observable cones and jets at each site. The high number of jets and the lack of observable cone and jet structures differ from the implications of the cone-jet mode; hence, the addition of the rim emission mode to the nomenclature. Precedent for this new mode definition can be found in the simple-jet to cone-jet differentiation.

Four addition works focused on a similar mode to study spray characteristics and spray mixing (Dunn and Snarski, 1991, 1992; Grace and Dunn, 1992; Snarski and Dunn, 1991). These works used ethanol at a flow rate of 6×10^{-3} ml s^{-1}. The electrical configuration was a prototypical capillary-plate configuration with a positive DC high voltage source. The authors reported droplet production from short ligaments originating at the capillary edge with no visible meniscus. The droplet size distribution was polydisperse, characteristic of multiple production sites. The droplet spray exhibited a rapid expansion near the production region characteristic of a high space charge region and the rim emission mode. The authors reported the spray as an electrohydrodynamic fine spray. In the present nomenclature, the spray probably operated in the rim emission mode.

3. PRESENTATION OF MODELS

This paper now turns to a discussion of EHDA modelling investigated in the literature. Several papers are reviewed for a brief discussion on the controlling parameters in EHDA. Focus has been on post-1990 works. This article does not attempt to review stability analyses of EHDA (of which there are many references). The purpose is simply to point out what models exists, report on the assumptions made and note what are the applicable EHDA modes. In some cases, comparisons with experimental data as reported by the individual authors are presented.

3.1. *Analytic models*

Eight models have been found that consider the effects of the parameters on EHDA in limited circumstances and are reviewed in the following. Of the eight, one concerns LMIS,

another does not consider the droplet production mechanism, *per se*, and the remaining six consider only the simple-jet or the cone-jet modes. These six are considered first.

Fernández de la Mora *et al.* (1990) relate the jet diameter to a $f(Q,\ \rho,\ \gamma)$ for an idealized, low electrical conductivity and low flow rate jet by neglecting the viscosity and the electrical acceleration terms in the steady-state momentum equation. A scaling analysis where the cube root of the ratio of the surface tension pressure to the dynamic pressure of the jet is of order one, leads to the momentum equation assumptions. The jet radius is then incorporated into the momentum equation through the relationship between the surface charge density and the normal electric field. The surface charge density is expressed in terms of Q, I and r_j by invoking charge conservation and assuming that the surface charge is convective and transported on a cylindrical surface. The assumption that the jet breaks up by varicose instabilities allows the jet diameter to be related to the droplet diameter ($d_j = 1.89\ d_d$). The authors report reasonable agreement between available experimental data and the predicted values for jet diameters (d_j) > about 5 μm.

Turnbull (1989) also models the jet breakup by varicose instability. Although this model predates 1990, it is reviewed because of the similarities to the above analysis and it is the basic reference for post-1990 jet stability analysis by its author. This model does not consider the breakup region, only the jet region where the diameter varies slowly with axial distance. As a result, the equations are linearized and written in steady state. It is assumed that the charged jet interacts with a ground electrode and no other electrical effects are present. Additionally, the jet velocity profile is assumed uniform, aerodynamic drag effects are neglected and the charge relaxation time is assumed to be sufficiently short relative to the fluid mechanical time such that the charge resides on the jet surface ($\sigma > 10^{-7}$ S m^{-1}). The model considers two limiting cases: a perfect conductor and a perfect insulator. The predicted jet diameter (for the perfectly insulating case — which is compared to experimental data) is expressed as a transcendental function, $f(Q,\ I,\ \rho,\ b,\ d_j)$, where b is the diameter of the ground electrode. Experimental results show that the calculations overpredict the jet diameter by a ratio of $\sim 2/3$. Droplet size is not explicitly discussed, but can be inferred. Additionally analyses by Turnbull (1991, 1992) consider the growth rates of the capillary instability on this type of jet using a perturbation scheme.

Kirichenko *et al.* (1990) balance the electrical, capillary (or surface tension) and viscous deformation pressures on a continuous, axial single-jet (simple-jet mode). The authors predict the spray current and report reasonable agreement with experiments through the mode range, especially for the range of low total electric field values where the nonlinearities due to the droplet space charge are not significant. The predicted current is shown to be functionally related to E, Q, σ, μ, γ, ρ, κ, g and the electrical geometry. No mention of the droplet size is made.

Verbitskii *et al.* (1991) derive the stability of emitted droplets based on the "principle of least dissipation of energy" for the cone-jet and simple-jet modes. The stability of emitted droplets is defined with respect to their self-charge (Rayleigh instability) and also with respect to the external electric field (Taylor instability). The least dissipation of energy minimizes the rate of change of free energy, not the final state. Breakup is assumed to take place by varicose instability and the droplet shape function for the surface energy term is based on experimental data from photographs of successive stages of droplet separation from the meniscus. The model is simplified to apply to perfectly conducting liquids, but it also applied with reasonable approximation to liquids with σ > about 10^{-2} S m^{-1}. Droplet diameters and charges are calculated from minimizing the energy dissipation equation with respect to the droplet diameter and charge. The resulting two equations contain an additional unknown function of the diameter, the Rayleigh criteria. The third equation for this system results from a force balance at the time of droplet separation from the meniscus. These three equations are solved simultaneously for the droplet diameter, charge and stability. The relationships are complicated functions of the droplet shape and fluid properties (σ, ρ). Numerical results predict that there exist ranges where emitted droplets are stable with respect to their self-charge and the electric field. These monodisperse regimes are traced as functions of ϕ and the hydrodynamic pressure. No reference data are presented.

Fernández de la Mora (1992) considers the space charge effects on the cone angle in the cone-jet mode. The spray charge distribution is idealized to preserve Taylor's scaling ($\phi \sim r^{1/2}$) for the spray as well as the cone. This idealization molds the spray into one with an angularly uniform droplet distribution constrained by a coordinate surface boundary and the origin located at the cone apex. The assumption on the spray boundary shape is experimentally shown to be reasonable near the apex and for very small droplets (<1 μm) where inertia can be neglected. Visual observations support this assumption down to the visual limit ($d<0.2$ μm), but there is no reason to expect significant deviations for much smaller droplets. The spray boundary is then treated as a droplet streamline, i.e., it has a zero normal electric field. The model approximates highly conductive fluids in an atmosphere and predicts the spray current to be on the order of $K_q\gamma$, where K_q is defined as the electrical mobility. The current, nondimensionalized by $K_q\gamma$, is then related solely to the cone semi-vertex angle (α). This model does not define α in terms of experimental conditions, e.g., ϕ or Q; however, for a given α consistent with experimental observations, the current predictions and spray angle show agreement to within 30% of experimental data.

Mestel (1994) presents two scaling models for non-polar liquids with $\varepsilon \sim \varepsilon_0$ in the cone-jet mode. Both models investigate a similarity solution for the fluid dynamics of the cone based on the electrical features of this mode. The models are strictly valid for the region far from the cone aperture and jet, although they can be extended to the jet region with reasonable results. These models are discussed in turn. The first model presents an inviscid, conical boundary layer approximation using a momentum integral approach. The cone angle varies from the Taylor angle and is related to the mass and charge flux. A large conduction current is assumed such that the tangential electric field inside the cone is much larger than the normal electric field. The cone is assumed to be at high Reynolds number. The dynamic pressure is then much larger than the surface tension pressure; hence, the electric stress is related to the Bernoulli pressure. The model predicts a cone angle as $f(I, \rho, \sigma, Q)$. Additionally, narrow cones generate less highly charged drops, i.e., the cone angle scales with the ratio I/Q. The results compare qualitatively to experiments, but quantitatively they differ by an order of magnitude.

The second model considers a thin, viscous boundary layer driven by tangential shear stress, where the normal and tangential electric fields inside the cone are comparable. It is assumed that the Taylor scaling for the surface charge density, i.e., the balance between the surface tension and the normal electric field, applies in a dynamic regime. The flow inside the cone beyond the boundary layer is not treated. The flow rate for this condition is electrostatically determined and the model predicts a unique flow rate dependent on fluid properties (γ, ρ, τ). This approximation agrees within a factor of 2 to 3 of experimental data. No prediction of the net current in this mode is made. The scaling applies to a distance r_c from the cone apex where the conical assumption breaks down and the jet is formed. The scaling analysis is extended into this region based on plausible arguments. Here, assuming that the net current will be on the order of the convective current where the conical shape breaks down ($r \sim r_c$) results in a current estimate as a function of ρ, γ, μ, and τ that underpredicts data by about a factor of five. The jet radius is similarly estimated in this breakdown region. This value again scales with ρ, γ, μ, and τ (but as a different function) and results in good agreement with data. The model predictions are compared to data drawn from the work of Hayati *et al.* (1986).

The remaining two models are now discussed. Kelly (1984a, b) presents a model relating the average droplet diameter of a spray to the spray charge density. In other words, the droplet diameter does not depend on the liquid properties. This is true for liquids in the "asymptotic spray regime" or Newtonian liquids with viscosities <250 (mPa s) and an average diameter >1 μm. The model is statistically based and seeks to maximize the system entropy. It does not explicitly consider the droplet production mechanism as the energy associated with droplet production is small relative to the total system energy. This model was derived well before 1990. It is included in this review as it is the only model that applies to noncone-jet modes. In fact, given satisfaction of the range limits, it is reported to satisfy any spray mode. Although the range limits are broad and cover a large part of the EHDA

data base, little data have been compared with this theory. The data reported by the author in the above two references for liquids of moderate to low conductivity ($\sigma < 10^{-6}$ S m^{-1}) do show a good prediction.

The last model has been derived for use with LMIS (Vladimirov *et al.*, 1993). This model predicts a droplet production mechanism from the Taylor cone (cone-jet mode) via two main mechanisms: a low frequency one (MHz) due to the mobility of the space charge near the meniscus apex and a high frequency one (GHz) due to Rayleigh instability. The low-frequency droplet production mechanism results from a repetition of the following cycle. The space charge modulates the electric field intensity at the production site, lowering the production frequency as the space charge increases. The lowered production frequency then allows a negative divergence of the charge carriers which lowers the internal electric field (due to the space charge) and, consequently, increases the production frequency. The high-frequency mechanism results from the Coulombic explosion or ejection of many daughter droplets from a parent droplet or surface that is charged to the Rayleigh limit. The predictions of this model agree well with the reported results on droplet charge-to-mass ratio and low-frequency production versus current level.

The applicability of the LMIS model to the EHDA process is not certain as the length scales are considerably smaller (d_j, d_d, L_j), the currents are appreciably higher (factor of about 10^1–10^2) and it predicts a polydisperse droplet size distribution. However, as stated in Section 2, LMIS fundamentally have similar controlling principles and should not be neglected from EHDA research. The high-frequency production rates predicted by this model are seen in the experiments reported by Meesters *et al.* (1992), Fernández de la Mora *et al.* (1990) and by Loscertales and Fernández de la Mora (1993). These works reported monodisperse size distributions; however, the production of polydisperse size distributions has not been rigorously discounted. Whether or not the proposed high-frequency mechanism is responsible for the experimentally observed high production frequency remains, at present, unknown. Many authors report droplet production on the low-frequency order (MHz), but for the cone-jet these are monodisperse populations.

The controlling parameter of EHDA is the total electric field intensity at both the droplet production region (meniscus apex, secondary jet tip, pinched region, etc.) and through the jet acceleration region. The parameters contributing to this field intensity include: the electrical geometry, the atmosphere, the electrical conductivity of the liquid (which itself depends on the liquid viscosity through the charge mobility), the space charge, the volumetric flow rate, the dielectric constant of the liquid, the liquid density and the surface tension. The volumetric flow rate influences the electric field intensity through the fluid mechanical residence time. This time needs to be considered in a ratio with the electrical relaxation time to understand the contribution. The dielectric constant of the liquid contributes through the electrical relaxation time, the density of the liquid partially defines the momentum of the jet and may be important. Finally, the liquid surface tension provides a counteractive force to the electrical force.

The spray mode, in general terms, depends on the balance of forces, i.e. the electric field intensity and the relative values of the parameters above. No model has been found to predict a given mode for a given parameter set.

3.2. *Numerical models*

The following paragraphs discuss three numerical studies on EHDA. What distinguishes these three from other numerical studies on the subject is: (1) they are post-1990, (2) they individually represent the three most common numerical methods (finite element, finite difference, Lagrangian simulation), (3) they model standard features of EHDA and have general applicability and, of course, (4) the familiarity of the current authors with these studies. The three studies are presented as samples of numerical techniques applied to EHDA and not intended as a review analogous to Sections 2 and 3.1.

Meesters (1992) used a commercial finite element software package to solve for the electric stress distributions on the surface of the liquid cone in the DAG mode. This model

incorporated the electrical configuration and assumed the cone as a fixed geometrical boundary surface. No space charge effects were incorporated. The reported results show that the electric field intensity, as calculated from the stress distribution, rapidly increases in both the tangential and normal directions towards the apex and that the resulting electric field intensity is high enough to initiate a corona discharge. The primary limitation of this method was that the space charge could not be incorporated. The fixed boundary surface is not a limitation, *per se*. Many numerical models for the shape of the cone in LMIS utilize essentially the same technique. A fixed boundary surface is first assumed and forces calculated. These forces are then used to generate a new boundary surface. Iterations on this process are often necessary. Examples of this technique can be found in, e.g., Forbes and Ljepojevic (1991b), Chung *et al.* (1991) and Kingham and Swanson (1984).

Grace (1993) modelled the droplet motion in the rim emission mode using finite difference equations. This model incorporated space charge effects but did not consider the droplet production mechanism and assumed a monodisperse size distribution. The reported results show qualitative prediction of the droplet velocity profiles, quantitative description of the spray expansion and regional separation of the internal and external electric field effects on droplet motion. The primary limitation of this model was the monodispersity assumption.

Gañán-Calvo *et al.* (1994) used a Lagrangian simulation to model droplet motion in the cone-jet mode under varicose breakup. The authors have shown the spray to be dilute, thus neglecting the aerodynamic coupling. The simulated spray was initially "seeded" with a log-normal droplet diameter distribution, droplet speeds equal to the jet speed in the breakup region, and initial droplet position randomly distributed about the jet breakup location. The jet speed resulted from a scaling analysis on the cone-jet assuming a conducting fluid, a cone angle approximately equal to the Taylor angle and no space charge effects. Space charge effects were accounted for in the Lagrangian simulation. The reported results show good predictions of droplet velocity profiles and the spray plume geometry. The predicted spatial segregation of droplet diameters matches experimental data. The model was limited by the low droplet number concentrations allowed and by neglecting the space charge effects on the droplet production.

4. SUMMARY

This paper investigated works on the subject of EHDA, focusing on 1990 to the present. Several extensive reviews had been conducted prior to 1990, but no summary of the current literature exists. This paper seeks to fill this need. Thirty-six articles on electrical atomization and 47 references in all were reviewed. The spray nomenclature suggested by Cloupeau and Prunet-Foch (1990) has been extended to include three new modes: the drop ejection mode, the rim emission mode and the DAG mode. Eight models have been reviewed and three numerical approaches are presented.

Several suggestions for future EHDA papers result from this review. These suggestions are intended to facilitate accurate and valid data comparisons between authors.

- Report liquid properties (σ, γ, μ, ρ, ϵ) and experimental configuration (electrical configuration, flow rate and flow source—either constant pressure or constant flow rate, and atmosphere).
- Use consistent units and scales to facilitate comparisons.
- Report the spray mode or a description of the observable character.
- Restrict benchmark experiments to the capillary-plate configuration to eliminate uncertainty in the total electric field calculations.

Suggestions for future work include the following:

- Determine the effect of space charge on the production region.
- Investigate the magnitude of the total electric field at the production site.
- Quantify the effects of the liquid properties on the spray through benchmark data acquisition.

— Derive a nondimensional parameter or parameters relating the external and internal variables to the spray characteristics.

The space charge warrants a great deal of attention in light of the effects on the spray where "no stable cone-jet was seen experimentally without the presence of space charge, either due to charged droplets, corona discharge or ion emission" (Joffre and Cloupeau, 1986).

REFERENCES

Bailey, A. I. (1988) *Electrostatic Spraying of Liquids.* Wiley, New York.
Balachandran, W., Ahmad, C. N. and Machowski, W. (1992) *Conf. Rec. IEEE- IAS* **2,** 1369.
Chung, M. S., Cutler, P. H., He, J. and Miskovsky, N. M. (1991) *Surface Sci.* **246,** 118.
Cloupeau, M. and Prunet-Foch, B. (1989) *J. Electrostatics* **22,** 135.
Cloupeau, M. and Prunet-Foch, B. (1990) *J. Electrostatics* **25,** 165.
CRC Handbook of Chemistry and Physics, 63rd Edition (1982). CRC Press, Boca Raton, FL.
Dunn, P. F. and Snarski, S. R. (1991) *Phys. Fluids A* **3,** 494.
Dunn, P. F. and Snarski, S. R. (1992) *J. appl. Phys.* **71,** 80.
Fernández de la Mora, J., Navascues, J., Fernandez, F. and Rossel Llompart, J. (1990) *J. Aerosol Sci.* **21,** (Suppl.) S673.
Fernández de la Mora (1992) *J. Fluid Mech.* **243,** 561.
Forbes, R. G. and Ljepojevic, N. N. (1991a) *Sprays and Aerosols* 1991 *Conf. Proc.,* Surrey, U.K.
Forbes, R. G. and Ljepojevic, N. N. (1991b) *Surface Sci.* **246,** 113.
Gañán-Calvo, A. M., Lasheras, J. C., Dávila, J. and Barrero, A. (1994) *J. Aerosol Sci.* **25,** 1121.
Gomez, A. and Tang, K. (1990) Paper presented at the Western States Section/The Combustion Inst. 1990 Fall Mtg.
Gomez, A. and Tang, K. (1994) *Phys. Fluids* **6,** 404.
Grace, J. M. (1993) Ph.D. Dissertation, Univ. of Notre Dame, IN
Grace, J. M. and Dunn, P. F. (1992) *Exp. in Fluids* **12,** 261.
Hayati, I., Bailey, A. I. and Tadros, Th. F. (1987) *J. Colloid Interface Sci.* (Parts I and II), **117,** 205.
Hiraoka, K. (1992) *Rap. Comm. Mass. Spectr.* **6,** 436.
Huebner, A. L. (1970) *Science* **168,** 118.
Jaworek, A. and Krupa, A. (1992) *Trans. Inst. Fluid Mach.* 155.
Joffre, G. H. and Cloupeau, M. (1986) *J. Electrostatics* **18,** 147.
Kelly, A. J. (1984a) *J. Inst. Energy,* **312,** 312.
Kelly, A. J. (1984b) *Aerosol Sci. Technol.* **12,** 526.
Kim, K. and Turnbull, R. J. (1976) *J. appl. Phys.* **47,** 1964.
Kingham, D. R. and Swanson, L. W. (1984) *Appl. Phys. A* **34,** 123.
Kirichenko, V. N., Shepelev, A. D., Polevov, V. N., Efimov, I. M., Golomuz, I. N., Yurov, Yu. L. and Academician Petryanov-Sokolov, I. V. (1990) *Sov. Phys. Dokl.* **35,** 1015.
Kozhenkov, V. I. and Fuks, N. A. (1976) *Russian Chem. Rev.* **45,** 1179.
Loscertales, I. G. and Fernández de la Mora, J. (1993) *Proc. Int. Workshop. Synth. Meas. Ultrafine Particles,* Delft, NL.
Lüttgens, U., Dülcks, Th. and Röllgen, F. W. (1992) *Surface Sci.* **266,** 197.
Marsh, J. F., Nunn, A. E. T. and Michelson, D. (1988) *J. Electrostatics* **20,** 313.
Meesters, G. M. H. (1992) Ph.D. Dissertation, Tech. Univ. Delft, Delft, NL.
Meesters, G. M. H., Vercoulen, P. H. W., Marjinissen, J. C. M. and Scarlett, B. (1992) *J. Aerosol Sci.* **23,** 37.
Mestel, A. J. (1994) *J. Aerosol Sci.* **25,** 1037.
Michelson, D. (1990) *Electrostatic Atomization.* Hilger, New York.
Michelson, D., Robbins, M. S. and Bradley, R. M. (1993) *J. Aerosol Sci.* **24,** (Suppl.) S491.
Pfeifer, R. J. and Hendricks, C. D. (1967) *Phys. Fluids* **10,** 2149.
Rulison, A. J. and Flagan, R. C. (1993) *Rev. Sci. Instrum.* **64,** 683.
Schweizer, J. W. and Hanson, D. N. (1971) *J. Colloid Interface Sci.* **35,** 417.
Shutov, A. A. (1991) *J. appl. Mech. Tech. Phys.* **32,** 162.
Smith, D. P. H., (1986) *IEEE Trans. IA,* **IA-22,** 527.
Snarski, S. R. and Dunn, P. F. (1991) *Exp. Fluids* **11,** 268.
Turnbull, R. J. (1989) *IEEE Trans. IA,* **25,** 699.
Turnbull, R. J. (1991) *Conf. Proc. IEEE-IAS A. Mtg.* 518.
Turnbull, R. J. (1992) *IEEE Trans. IA* **28,** 1432.
Vercoulen, P. H. W., Camelot, D. M. A., Marijnissen, J. C. M., Pratsinis, S. and Scarlett, B. (1993) *Proc. Int. Workshop. Synth. Meas. Ultrafine Particles,* Delft, NL.
Verbiskii, S. S., Grigor'ev, A. I., Zemskov, A. A. and Shiryaeve, S. O. (1991) *Fluid Dynamics* **26**(2), 183.
Vladimirov, V. V., Badan, V. E., Gorshkov, V. N. and Soloshenko, I. A. (1993) *App. Surface Sci.***65/66,** 1.
Wang, S. H., Chang, J. S. and Berezin, A. A. (1993) *J. Electrostatics* **30,** 235.